

Bisecting GlcNAc is a general suppressor of terminal modification of *N*-glycan

Miyako Nakano¹, Sushil K. Mishra^{2,3}, Yuko Tokoro⁴, Keiko Sato⁵, Kazuki Nakajima⁶, Yoshiki Yamaguchi^{3,7}, Naoyuki Taniguchi^{5,8} & Yasuhiko Kizuka^{4,5,*}

¹Graduate School of Advanced Sciences of Matter, Hiroshima University, 1-3-1 Kagamiyama, Higashihiroshima, Hiroshima 739-8530, Japan.

²Glycoscience Group, National University of Ireland, Galway, Ireland.

³Structural Glycobiology Team, RIKEN-Max Planck Joint Research Center, Global Research Cluster, RIKEN, 2-1 Hirosawa, Wako, Saitama 351-0198, Japan.

⁴Center for Highly Advanced Integration of Nano and Life Sciences (G-CHAIN), Gifu University, 1-1 Yanagido, Gifu 501-1193, Japan.

⁵Disease Glycomics Team, RIKEN-Max Planck Joint Research Center, Global Research Cluster, RIKEN, 2-1 Hirosawa, Wako, Saitama 351-0198, Japan.

⁶Division of Clinical Research Promotion and Support, Center for Research Promotion, Fujita Health University, 1-98 Dengakugakubo, Kutsukake-cho, Toyoake, Aichi 470-1192, Japan.

⁷Synthetic Cellular Chemistry Laboratory, RIKEN, 2-1 Hirosawa, Wako, Saitama 351-0198, Japan.

⁸Department of Glyco-Oncology and Medical Biochemistry, Osaka International Cancer Institute, 3-1-69 Otemae, Chuoku, Osaka 541-8567, Japan.

*Correspondence to: Yasuhiko Kizuka (kizuka@gifu-u.ac.jp). Center for Highly Advanced Integration of Nano and Life Sciences (G-CHAIN), Gifu University, 1-1 Yanagido, Gifu 501-1193, Japan. Tel: +81-58-293-3356.

Running title: Bisecting GlcNAc suppresses *N*-glycan terminal modifications

The abbreviations used are:

AAL, *Aleuria aurantia* lectin

AD, Alzheimer's disease

E4-PHA, erythroagglutinating phytohemagglutinin

ER, endoplasmic reticulum

Fuc, fucose

Gal, galactose

GlcA, glucuronic acid

GlcNAc, N-acetylglucosamine

GluA2, AMPA-type glutamate receptor-2

GGnGGnbi, Gal-terminated biantennary

GnGnbi, GlcNAc-terminated biantennary

GnT, N-acetylglucosaminyltransferase

Hex, hexose

HNK-1, human natural killer-1

LacNAc, N-acetyllactosamine

Le, Lewis

MD, molecular dynamics

Man, mannose

MAM, *Maackia amurensis* lectin

NCAM, neural cell adhesion molecule

PA, pyridylamine

PhoSL, *Pholiota squarrosa* lectin

RMSF, root mean square fluctuations

Sia, sialic acid

SSA, *Sambucus sieboldiana* lectin

ABSTRACT

Glycoproteins are decorated with complex glycans for protein functions. However, regulation mechanisms of complex glycan biosynthesis are largely unclear. Here we found that bisecting GlcNAc, a branching sugar residue in *N*-glycan, suppresses the biosynthesis of various types of terminal epitopes in *N*-glycans, including fucose, sialic acid and human natural killer-1. Expression of these epitopes in *N*-glycan was elevated in mice lacking the biosynthetic enzyme of bisecting GlcNAc, GnT-III, and was conversely suppressed by GnT-III overexpression in cells. Many glycosyltransferases for *N*-glycan terminals were revealed to prefer a non-bisected *N*-glycan as a substrate to its bisected counterpart, whereas no upregulation of their mRNAs was found. This indicates that the elevated expression of the terminal *N*-glycan epitopes in GnT-III-deficient mice is attributed to the substrate specificity of the biosynthetic enzymes. Molecular dynamics simulations further confirmed that non-bisected glycans were preferentially accepted by those glycosyltransferases. These findings unveil a new regulation mechanism of protein *N*-glycosylation.

INTRODUCTION

Protein glycosylation is the most abundant post-translational modification (1). Glycan structures even on a single glycoprotein are diverse, and protein functions are dynamically regulated by their specific glycosylation states (2, 3). Indeed, alteration of or dynamic changes to the glycan structures on proteins affect various physiological processes, such as protein folding, stability, trafficking and activity (2, 3). Furthermore, genetic deletion of particular glycans in mice improved or accelerated the pathology of various diseases including cancer, Alzheimer's disease (AD), diabetes and muscle dystrophy (4-7). For example, loss of β 1,6-branch of *N*-glycan improves cancer, where loss of another branch (β 1,4-branch) of *N*-glycan causes type-2 diabetes. In human patients, aberrant expression of disease-relevant glycans promoted and affected pathogenesis (3, 8, 9), indicating that changes to glycan structures represent a direct target for disease diagnosis and therapy. However, there is a paucity of information describing the detailed mechanisms of how complex glycan structures are dynamically formed in living cells.

N-glycans are highly conserved and abundant, and expressed on most proteins that pass through the secretory pathway (10). Although the early biosynthetic system of *N*-glycans that occurs in endoplasmic reticulum (ER) is highly conserved among all eukaryotic cells (10), the biosynthesis of later phases of *N*-glycans in the Golgi apparatus is very diverse and is regulated in a protein-selective manner, leading to a wide variety of *N*-glycan structures on glycoproteins. The major structural diversity of *N*-glycans is the presence or absence of various GlcNAc branches synthesized by *N*-acetylglucosaminyltransferases (GnTs encoded by *MGAT* genes) (Supplemental Fig. S1). Each sugar branch can be further decorated with various types of terminal modifications such as *N*-acetyllactosamine (LacNAc), LacdiNAc, α Gal, sialic acid, Lewis (Le)-type fucose and human natural killer-1 (HNK-1) (Fig. 1A and 2A) (11). Biochemical studies showed that branch formation basically precedes the biosynthesis of terminal modifications (11). Final *N*-glycan structures on each glycoprotein or even a single *N*-glycosylation site are biosynthesized by concerted and competitive actions of various glycosyltransferases in the Golgi, but how the actions of these glycosyltransferases are regulated in the Golgi remains to be elucidated.

Bisecting GlcNAc, the central branch of *N*-glycan expressed highly in brain and kidney, is biosynthesized by a glycosyltransferase GnT-III (encoded by the *MGAT3* gene) (Fig. 1A) (12) and was reported to be associated with several diseases. *Mgat3*-deficient mice showed improved AD pathology with reduced amyloid-plaque formation in brain (4, 13, 14). This was found to be caused by relocation of a key amyloid-producing enzyme, beta-site APP-cleaving enzyme-1 (BACE1), from early endosomes to lysosomes (4). Furthermore, overexpression of GnT-III in B16 melanoma cells resulted in the prevention of lung metastasis in mice, probably through regulation of membrane retention of E-cadherin (15, 16), whereas *Mgat3*-deficient mice showed rapid growth and early metastasis of breast cancer (17). These *in vivo* studies showed that the presence or absence of bisecting GlcNAc has a significant impact on the development of these diseases by regulating the functions of target glycoproteins. In addition, bisecting GlcNAc has unique biochemical features when compared with other GlcNAc branches. Previous enzymatic studies revealed that glycans with bisecting GlcNAc are no longer substrates of other glycosyltransferases (18-20), including GnT-IV (21) and GnT-V (22). In addition, bisecting GlcNAc does basically not undergo further elongation by other sugar residues (Gal and Sia) (11, 23), whereas other GlcNAc branches are usually linked to other sugar residues. Moreover, previous simulation and structural studies indicated that the presence of bisecting GlcNAc substantially changed the preferable conformations of whole *N*-glycans (24-26), suggesting that the presence of a bisecting GlcNAc residue itself, but not its elongation, is important for the function of bisecting GlcNAc. These results indicate that bisecting GlcNAc uniquely affects the tertiary structure and biosynthesis of whole *N*-glycans, which modulates the function of target glycoproteins. However, it is unclear how bisecting GlcNAc affects the biosynthesis of *N*-glycan structures *in vivo*.

In this study, to understand whether bisecting GlcNAc regulates whole *N*-glycan structures, we carried out *N*-glycomic and biochemical analysis of *Mgat3*-deficient mouse brain. We found significant increases in various terminal modifications of *N*-glycans, including Le-type fucose, sialic acid and the HNK-1 epitope. We also reveal that most glycosyltransferases acting on *N*-glycan terminals have lower preference toward bisected glycans as substrates over non-bisected glycans, which was further supported by our docking models and molecular dynamics (MD) simulations. These data indicate that

bisecting GlcNAc serves as a general suppressor of various terminal modifications of *N*-glycans, highlighting its importance for fine regulation of glycan structures on proteins.

EXPERIMENTAL PROCEDURES

Antibodies and lectin

Commercially available antibodies used were as follows: anti-ST6GAL1 (M2, 28047) was from Immuno-Biological Laboratories (Japan), anti-VDAC1 (ab14734) from Abcam, anti-actin (A4700) from Sigma, anti-GAPDH (MAB374) and anti-myc (4A6, 05-724) from Millipore, anti-polysialic acid (12E3, 14-9118-80) from Thermo Fisher Scientific, anti-HNK-1 (559048) from BD Biosciences, anti-beta-III-tubulin (tuj1, MMS-435P) from Covance and anti-myc (9E10, BML SA-294) from Enzo Life Sciences. Biotinylated *Aleuria Aurantia* Lectin (AAL) (J201-R), erythroagglutinating phytohemagglutinin (E4-PHA) lectin (J211), *Sambucus sieboldiana* (SSA) (J218), *Maackia amurensis* (MAM) (J210) were from J-Chemical. The biotinylated *Pholiota squarrosa* lectin (PhoSL) was provided by J-Chemical. The anti-GnT-III (clone 33A8) was provided by Dr. Eiji Miyoshi (Osaka University). The anti-GlcAT-P (GP2) was provided by Dr. Shogo Oka (Kyoto University). The anti-Sialyl Le^x (F2) was provided by Dr. Hiroto Kawashima (Chiba University).

Mutant mice

The generation of the *Mgat3*-deficient mice has been described previously (27). All mice were from a C57BL/6 genetic background. *Mgat3*-deficient mice were generously provided by Dr. Jamey D. Marth (University of California-Santa Barbara). Mice were housed (three or fewer mice per cage) at $23 \pm 3^{\circ}\text{C}$ and $55 \pm 10\%$ humidity. The light condition was 14 h : 10 h (lights on at 7:00). All animal experiments were approved by the Animal Experiment Committee of RIKEN and Gifu University.

Plasmids

The construction of pcDNA6-mycHisA/mouse FUT1, FUT2, FUT4 and FUT9 to express C-terminally myc-tagged full-length fucosyltransferases was described previously (28). Mouse FUT7 cDNA was amplified by PCR by using a mouse liver cDNA library and then ligated into pCR-Blunt (ThermoFisher Scientific). By using pCR-Blunt/mouse FUT7 as a template, FUT7 cDNA was amplified and subcloned into the EcoRI/XhoI site of pcDNA6-mycHisA to express C-terminally myc-tagged FUT7. Human GnT-III (*MGAT3*) cDNA was amplified by using pCXN2/human GnT-III (29) as a template and cloned into the EcoRI/XbaI site of pcDNA6-mycHisA to construct a plasmid for C-terminally myc-tagged GnT-III. A cDNA encoding the inactive rat GnT-III^{D321A} mutant was amplified by PCR using pCXN2/rat GnT-III^{D321A} (gift from Dr. Tomoya Isaji, Tohoku Medical and Pharmaceutical University) as a template, followed by insertion into the EcoRI/XhoI site of pcDNA6-mycHisA. pcDNA3.1/rat ST6GAL1-FLAG was provided by Dr. Shinobu Kitazume (Fukushima Medical University) (30). A cDNA encoding human ST3GAL4 was amplified by PCR using pSVL/human ST3GAL4-FLAG (STZ) (Dr. Hiroshi Kitagawa, Kobe Pharmaceutical University) as a template and cloned into the EcoRI/XhoI site of pcDNA6-mycHisA to construct a plasmid for C-terminally myc-tagged full-length ST3GAL4. cDNAs encoding the catalytic domains of human GnT-III (from Glu63 to Val533), human ST3GAL4 (from Glu43 to Phe332) and ST6GAL1 (from Lys98 to Cys406) were amplified and ligated into the EcoRI/EcoRV site (for GnT-III) or EcoRI/XhoI site (for ST3GAL4 and ST6GAL1) of pcDNA-IH (28) that contains DNA encoding the Igk signal peptide and 6xHis tag. ProteinA-tagged B4GALT1 (31), proteinA-tagged GlcAT-P (32), and full-length GlcAT-P (pIRES/rat GlcAT-P and rat HNK-1ST) (33) were kindly provided by Dr. Shogo Oka (Kyoto University). The primers used for construction are listed in Supplemental Table S1.

Glycan analysis of mouse brain

N-Glycans from brain membranes were released (34), labelled with aminoxymethylamine (TMT6 reagent (ThermoFisher Scientific) and analyzed by LC-ESI MS, according to previous procedures (35, 36) with modifications as follows.

Mouse brains (30 mg) were crushed in 2 mL of homogenization buffer (50 mM Tris-HCl, pH 7.4, 0.1 M NaCl, 1 mM EDTA and protease inhibitor cocktail (Roche)) using a Dounce tissue grinder and then homogenized using a polytron homogenizer, followed by centrifugation at 760 x g for 20 min at 4°C to remove nuclei and unbroken cells. The supernatant was diluted with 2 mL of Tris-buffer (50 mM Tris-HCl, pH 7.4, 0.1 M NaCl) and then ultracentrifuged at 120,000 x g for 80 min at 4°C. The membrane pellet was suspended in 100 µL of the Tris-buffer, followed by addition of 400 µL of the Tris-buffer containing 1% Triton X-114 with pipetting. The lysate was incubated on ice for 10 min and then at 37 °C for 20 min, followed by phase partitioning by centrifugation at 1,940 x g for 2 min. The upper aqueous phase was removed, and the lower detergent phase was mixed with 1 mL of ice-cold acetone and kept at -25°C overnight. After centrifugation at 1,940 x g for 2 min, the precipitated membrane proteins were dissolved with 11 µL of 8 M Urea and spotted (2.5 µL x 4 times) onto an ethanol-pretreated PVDF membrane. After drying at room temperature for > 4 hours, the membrane was washed with ethanol for 1 min once and then with water for 1 min three times. The protein on the membrane was stained for 5 min with Direct Blue 71 (Sigma Aldrich) (800 µL solution A (0.1% Direct Blue 71) in 10 mL solution B (acetic acid:ethanol:water = 1:4:5)). After destaining with solution B for 1 min, the membrane was dried at room temperature for > 3 h. The protein spots were excised from the membrane and placed into a well of a 96-well plate. The spots were covered with 100 µL of 1% (w/v) poly(vinylpyrrolidone) 40000 in 50% (v/v) methanol, agitated for 20 min and washed with water (100 µL x 5 times). PNGase F (2U in 10 µL of 20 mM phosphate buffer, pH 7.3, Roche) was added to the well and the spots were incubated at 37 °C for 15 min, followed by the addition of 10 µL of water and incubated at 37°C overnight. The samples were sonicated (in the 96-well plate) for 10 min and the released *N*-glycans (20 µL) were transferred to 1.5-mL polypropylene tubes. The well was washed with water (50 µL twice), and the washings were combined and evaporated.

The dried *N*-glycans were reacted with aminoxymethylamine (TMT6 reagent (Thermo Fisher Scientific, 0.02 mg in 200 µL of 95% methanol, 0.1% acetic acid solution) by continuous shaking for 15 min at room temperature. After evaporating the reaction solution, 200 µL of 95% methanol was added to the samples, followed by further shaking for 15 min. After evaporating the samples, 100 µL of 10% acetone

solution was added to the samples, followed by incubation at room temperature for 15 minutes with continuous shaking. The sample was evaporated and excess reagent was removed using Sepharose CL4B. The samples were dried, dissolved with 20 μ L of 10 mM ammonium bicarbonate and analyzed by LC-ESI MS/MS. *N*-Glycans labelled with aminosyTMT6 were separated on a carbon column (5 μ m HyperCarb, 1 mm I.D. x 100 mm, Thermo Fisher Scientific) using an Accela HPLC pump (flow rate: 50 μ L/min) under the following gradient conditions; a sequence of isocratic and two segmented linear gradients: 0–8 min, 10 mM NH_4HCO_3 ; 8–38 min, 9–22.5% (v/v) CH_3CN in 10 mM NH_4HCO_3 ; 38–73 min, 22.5–51.75% (v/v) CH_3CN in 10 mM NH_4HCO_3 ; and increasing to 81% (v/v) CH_3CN in 10 mM NH_4HCO_3 for 7 min and re-equilibrated with 10 mM NH_4HCO_3 for 15 min. The eluate was introduced continuously into an ESI source (LTQ Orbitrap XL, Thermo Fisher Scientific). MS spectra were obtained in the positive ion mode using Orbitrap (mass range: m/z 800 to m/z 2000; capillary temperature: 300°C; source voltage: 4.5 kV; capillary voltage: 18 V; tube lens voltage: 110 V). For MS/MS analysis, the top three precursor ions were fragmented by HCD using a stepped collision energy (normalized collision energy: 35.0; the width: 40.0; the steps: 3; minimum signal required: 10000; isolation width: 4.00; activation time: 100) using Orbitrap. Monoisotopic masses were assigned with possible monosaccharide compositions using the GlycoMod software tool (mass tolerance for precursor ions is ± 0.005 Da, <https://web.expasy.org/glycomod/>) and the proposed glycan structures were further verified through annotation using a fragmentation mass matching approach based on the MS/MS data. Xcalibur software ver. 2.2. (Thermo Fisher Scientific) was used to show the base peak chromatogram (BPC), extracted ion chromatogram (EIC) and to analyze MS and MS/MS data. The relative abundances (%) of each glycan structures were calculated by setting the total peak intensities of oligomannose-type *N*-glycans in each EIC as 100%.

Preparation of membrane and soluble fractions from mouse brain

Mouse brains were homogenized using a Potter-type tissue grinder with seven volumes of TBS containing an EDTA-free protease inhibitor cocktail (Roche). Homogenates were ultracentrifuged at

105,000 × g for 30 min at 4°C, and the supernatant and pellet were used as soluble and membrane fractions, respectively.

Western and lectin blotting

These experiments were performed as described previously (35). Signals were detected using ImageQuant LAS-4000mini (GE Healthcare) or FUSION SOLO.7S (VILBER). The intensity of the protein bands was quantified using ImageQuant TL (GE Healthcare) or ImageJ software.

Immunofluorescence staining

Twenty-week-old mice were transcardially perfused with PBS containing 1 U/ml heparin sodium followed by 4% paraformaldehyde in PBS. Brains were taken and sequentially immersed in the same fixative overnight and then in 30% sucrose in PBS for 3 d (with daily renewal of the buffer) at 4°C. Brain sections (30 µm thick) were stained using the floating method. Briefly, sections were incubated with PBS containing 3% BSA for 20 min at room temperature, followed by incubation with primary antibody (1 h at room temperature) and Alexa-labelled secondary antibody (30 min at room temperature). Fluorescence was visualized using an Olympus FV-1000 confocal microscope.

Preparation of primary neurons

Primary cortical were isolated from mouse embryos as described previously (4). At DIV2, Ara-C (C6645, Sigma) was added to a final concentration of 5 µM to kill dividing non-neuronal cells. Half the amount of medium was replaced with new one every 5 d, and the cells were collected at DIV15.

RNA extraction, reverse-transcription and quantitative PCR

Total RNA from mouse brain was extracted using the TRI-REAGENT (Molecular Research Center). Reverse-transcription and qPCR were performed by using Qiagen reagents and 96 well-based primers

of glycosyltransferases as described previously (37). The expression levels of glycosyltransferases relative to those of *Actb*, *B2m*, *Gapdh* and *Hsp90ab1* were calculated by the Δ Ct method. For quantification of the single gene mRNA (*Mgat3*), reverse-transcription and qPCR were performed using Superscript III and TaqMan probes as described previously (38).

Analysis of nucleotide sugars

Mouse brains (11-week-old) were obtained after the focused microwave irradiation technique to eliminate biochemical artefacts resulting from post-mortem degradation of nucleotide sugars. We therefore subjected mice to high-energy focused beam microwave irradiation (5 kW, 0.94 s; MMW-05 Muromachi Kikai, Tokyo). The brains were then taken at room temperature, frozen in liquid nitrogen and stored at -80°C (39).

Nucleotide sugars were prepared and quantified by ion-pair reversed-phase LC-MS as described previously (40, 41). The nucleotide sugar levels in brain tissues were normalized by the recovery of exogenous GDP-Glc and indicated as pmol/mg protein.

Cell culture and transfection

Cell lines were maintained and transfected as described previously (35). COS7, HEK293, and Hela cells were cultured in DMEM supplemented with 10% FBS. CHO cells were maintained in MEM α supplemented with 10% FBS. For knockdown experiments, cells at 20-40% confluency on 6-cm dishes were transfected with 80 pmol of control siRNA (AllStars negative control siRNA, QIAGEN) or siRNA for *MGAT3* (SI00631022) using 8 μ l of Lipofectamine 2000.

Expression and purification of recombinant glycosyltransferases

Expression and purification of recombinant glycosyltransferases were performed basically as described previously (28, 31, 35). For preparing FUT1-, FUT2-, FUT4-, or FUT9-myc, COS7 cells were

transfected with each plasmid with Polyethyleneimine MAX. After 48 h, cells were lysed with TBS containing 1% Nonidet P-40 (NP-40) and protease inhibitors, followed by centrifugation at 20,000 x g. The anti-myc antibody (4A6) and Dynabeads Protein G (Invitrogen) were added to the supernatant, followed by gentle rotation at 4°C overnight. The beads were washed with TBS containing 0.1% NP-40 three times and suspended with TBS containing 0.1% NP-40. The beads suspension was used directly for enzyme assays.

For preparing His-tagged GnT-III, ST6GAL1 and ST3GAL4, and proteinA-tagged GlcAT-P and B4GALT1, COS7 cells were transfected with each plasmid and Polyethyleneimine MAX, followed by replacement of the medium with Opti-MEM I (GIBCO) at 4-6 h post-transfection. After 3-4 days, recombinant enzymes were purified from the media through a Ni²⁺- or IgG-column. For His-tagged enzymes, the bound proteins were eluted from the Ni²⁺-column with 20 mM phosphate buffer, pH 7.2, containing 0.5 M imidazole and 0.5 M NaCl, and then desalted with a NAP-5 column (GE Healthcare) equilibrated with 50 mM MES pH 6.2. For proteinA-tagged enzymes, the bound proteins were eluted from the IgG-column with 100 mM glycine, pH 2.5, and then immediately neutralized with 1 M Tris-HCl, pH 8.5.

Preparation of PA-labelled sugars

GnGnbi-PA was prepared as described previously from egg yolk sialylglycopeptide (Fushimi Pharmaceutical) by releasing *N*-glycans with PNGase F, labelling with 2-aminopyridine, and treating with sialidase and galactosidase (42). To prepare GGnGGnbi-PA (type-2 galactosylated form of GnGnbi-PA), GnGnbi-PA was incubated with purified proteinA-B4GALT1 in 125 mM MES pH 6.2, 10 mM MnCl₂, 10 mM UDP-Gal at 37°C overnight. To prepare bisected type GGnGGnbi-PA (bisectGGnGGnbi-PA), GnGnbi-PA was first incubated with purified His-GnT-III in 125 mM MES pH 6.2, 10 mM MnCl₂, and 20 mM UDP-GlcNAc, at 37°C for 1 h, and then the reaction products were further galactosylated by adding purified proteinA-B4GALT1 and UDP-Gal (10 mM at final concentration) at 37°C overnight. The products were separated and purified through reverse-phased HPLC equipped with a TSK-gel ODS-80TM (4.6 x 150) column (TOSOH), and the retention times of

the products were confirmed to be the same as standards (TAKARA BIO). The purity and mass number of the purified products were confirmed by MALDI-TOF MS (Ultraflex, Bruker Daltonics).

Glycosyltransferase assays

Glycosyltransferase activity was measured as described previously (42) with modifications. Activity assays were performed using myc-tagged full length FUT1, FUT2, FUT4, FUT9, or His-tagged soluble ST6GAL1, ST3GAL4, or proteinA-tagged soluble GlcAT-P. These enzymes were expressed in COS7 cells, affinity purified, and incubated with acceptor substrates (GGnGGnbi-PA or bisectGGnGGnbi-PA) in 125 mM MES pH 6.2, 10 mM MnCl₂, 0.2 M GlcNAc, 0.5% Triton X-100, 1 mg/ml BSA and donor substrates. As donor substrates, 1 mM GDP-Fuc, 1 mM CMP-NeuAc, and 2 mM UDP-GlcA were used for fucosyltransferase, sialyltransferase, and glucuronyltransferase, respectively. The reaction products were analyzed by reversed-phase HPLC equipped with a TSK-gel ODS-80TM (4.6 x 150) column (TOSOH). Isocratic mobile phase (A, 20 mM ammonium acetate pH 4.0; B, 20 mM ammonium acetate pH 4.0 containing 1% 1-butanol) was used, and the appropriate buffer B contents were adjusted for each enzyme assay.

Modelling of N-glycans with GlcAT-P and ST6GAL1

We modelled the binding modes of biantennary (GGnGGnbi) and bisected biantennary (bisectGGnGGnbi) glycans using computational modelling. We extracted the starting structure of GGnGGnbi from the *N*-glycosylation site of human ST6GAL1 crystal structure (PDB ID: 4js1) (43). bisectGGnGGnbi structure was created manually by adding bisecting GlcNAc to GGnGGnbi. Structures of the human GlcAT-P (PDB ID: 1v82) (44) and ST6GAL1 (PDD ID: 4js1) (43) were taken from the Protein Data Bank. The GlcAT-P/*N*-Glycan complexes were created by pair fitting Gal β 1,4GlcNAc from the α 1,3-branch over the Gal β 1,4GlcNAc fragment in the crystal structure of the human GlcAT-P (α 1,3-binding mode). Molecular docking was performed because the glycan fragment in the ST6GAL1 active site was absent in the crystal structure. Docking of full *N*-glycans to ST6GAL1

resulted in very unreasonable binding conformations because of its large size and unusual flexibility along the glycosidic linkages. Thus, we performed molecular docking of the *N*-glycan branch alone (Gal β 1,4GlcNAc β 1,2Man α) in ST6GAL1 using Vina-Carb software (45). A total of 100 binding modes were generated. The top scoring pose displayed a reasonable binding conformation where the O6 hydroxyl of the terminal galactose is accessible to cytidine-5' monophosphate (CMP) in the ST6GAL1 crystal structure (PDB ID: 4s02). The ST6GAL1/*N*-Glycan complex structures were then created by pair fitting Gal β 1,4GlcNAc of the α 1,3-branch over the docked Gal β 1,4GlcNAc fragment. The modelled complex looked similar to that shown in Fig. 2C of Kuhn et al. (43).

These complexes were further subjected to classical MD simulations. All four complexes were solvated in an octahedral TIP3P water box extending 12 Å from each side of the complex. Amber force field ff14SB31 was used to treat the protein, whereas GLYCAM06 (version j-1) was used for glycans. The Li/Merz ion parameters were used for the Mn²⁺ ion in the GlcAT-P active site (46). Complexes were first equilibrated using a multi-step biomolecular equilibration protocol (47). A production run (200 ns in each case) under an NPT ensemble was performed using the *pmemd* (cuda version) module of Amber14 (48). Other MD settings (2 fs time step; 300 K constant temperature control using the weak coupling algorithm) were similar to that of a previous study (47). All MD trajectories were analyzed using AmberTools18 (<http://ambermd.org>). *N*-glycan binding conformations were clustered into three clusters using the *K-means* clustering approach implemented in *cpptraj*. A representative conformation from the most populated cluster was used in further analysis and figures. The *N*-glycan conformations in MD were also analyzed by calculating free-energy plots of the orientation of the α 1,6-glycosidic linkage in spherical coordinates as reported by Nishima et al. (49) (Supplemental Fig. S7B-F). The distribution of essential conformers of the biantennary glycans are named as back-fold, tight back-fold, extended A and parallel. The parallel conformation is the one where the α 1,6-branch is arranged parallel to the α 1,3-branch.

Experimental Design and Statistical Rationale

For all MS and blotting experiments, at least 3 independent pairs of *Mgat3*^{+/+} and *Mgat3*^{-/-} littermates were used, and the representative data are shown in Figures. All data are shown as means ± SEM. For comparison of the means between two groups, statistical analysis was performed by applying an unpaired one-sided Student's *t*-test or Mann-Whitney U-test. *p* values less than 0.05 were considered to be significant.

RESULTS

Increases in terminal modifications of N-glycans in Mgat3^{-/-} brain

To determine whether bisecting GlcNAc affects the biosynthesis of other parts of *N*-glycans, *N*-glycan structures of *Mgat3*^{+/+} and *Mgat3*^{-/-} mouse brains were analyzed by liquid chromatography (LC)-mass spectrometry (MS)/MS (Fig. 1B and Supplemental Fig. S2). Reducing ends of *N*-glycans were labeled with TMT6, and analyzed by LC-MS/MS in positive ion mode, which allows various glycans to be detected with high sensitivity in MS. We first found that *N*-glycans with bisecting GlcNAc and deduced to have bisecting GlcNAc disappeared in *Mgat3*^{-/-} brain (Fig. 1B and Supplemental Fig. S2, indicated in blue). Glycan structures with bisecting GlcNAc were assigned based on the diagnostic ions for bisecting GlcNAc (Supplemental Fig. S2D) which were confirmed to be completely absent in *Mgat3*^{-/-} brain (Supplemental Fig. S2F). These results indicate that GnT-III is the sole biosynthetic enzyme of bisecting GlcNAc in mammals, which is consistent with a previous report (50). We also found that the levels of many glycans were increased in *Mgat3*^{-/-} brain (Fig. 1B and Supplemental Fig. S2, indicated in red), and surprisingly, the number of fucose and sialic acid residues in these increased glycans were higher than those found in the *N*-glycans that had decreased in *Mgat3*^{-/-} brain. Here, the sum of signal intensity of multi-fucosylated glycans in MS analysis was greatly higher in *Mgat3*^{-/-} than in *Mgat3*^{+/+}, whereas that of mono-fucosylated glycans was reduced in *Mgat3*^{-/-} brain to less than 50% of that in *Mgat3*^{+/+} (Fig. 1C, left). Similar increases in mono- and multi-sialylated glycans in *Mgat3*^{-/-} was clearly observed (Fig. 1C, right). Moreover, extracted ion chromatogram (EIC) analysis of diagnostic ions for

LeY or LeA (658.256) and sialyl Le (803.294) showed that glycans having these epitopes were observed only in *Mgat3*^{-/-} samples. These data suggest that fucosylation and sialylation in *N*-glycans are enhanced in *Mgat3*^{-/-} brain. Consistent with the MS results, lectin blotting showed that proteins from *Mgat3*^{-/-} brains were stained more strongly with *Aleuria aurantia* lectin (AAL), which recognizes all fucose residues (51), than those from *Mgat3*^{+/+} brain (Fig. 1D, 1st panel). Although mammalian *N*-glycans are potentially fucosylated at both core and terminal positions (Fig. 1A), unaltered staining between *Mgat3*^{+/+} and *Mgat3*^{-/-} brains with core-fucose-specific *Pholiota squarrosa* lectin (PhoSL) (52) (Fig. 1D, 2nd panel) suggests that Le-type fucosylation but not core fucosylation is enhanced in *Mgat3*^{-/-} brain. We also observed that α 2,6-sialylation and α 2,3-sialylation were increased slightly in *Mgat3*^{-/-} brain in lectin blots with *Sambucus sieboldiana* lectin (SSA) and *Maackia amurensis* lectin (MAM), respectively (Fig. 1E, left and middle panels). The absence of bisecting GlcNAc in *Mgat3*^{-/-} brain was also confirmed by the loss of signals with bisecting GlcNAc-reactive lectin, erythroagglutinating phytohemagglutinin (E4-PHA) (Fig. 1E, right panel). Collectively, the MS and lectin blotting data showed that terminal fucosylation and sialylation increased in *Mgat3*^{-/-}, suggesting that bisecting GlcNAc has a negative impact on the biosynthesis of these terminal structures in *N*-glycans.

We next examined the levels of other terminal modifications of *N*-glycans, which cannot be detected by conventional MS analysis, such as HNK-1 and polysialic acid (polySia) (Fig. 2A and Supplemental Fig. S1B). These glycan epitopes are expressed at *N*-glycan terminals specifically in brain and play key roles in neural functions, including learning, synaptic formation and neurological disorders (53-55). Western blotting and immunostaining of adult mouse brains with HNK-1 mAb showed that the levels of the HNK-1 epitope increased in *Mgat3*^{-/-} brain (Fig. 2B, C). The expression levels of neural cell adhesion molecule (NCAM) and AMPA-type glutamate receptor-2 (GluA2), the major carrier proteins of HNK-1 glycan (53), were comparable in *Mgat3*^{+/+} and *Mgat3*^{-/-} mice (Fig. 2B), indicating that the levels of HNK-1 glycan but not its carrier proteins were upregulated in *Mgat3*^{-/-} brain. PolySia is highly expressed in nascent brain (55), and its expression is downregulated with age and persists in very restricted areas of adult brain, such as the hippocampus. Western blotting of neonatal (P0) mouse brains and primary cerebral neurons (DIV15 isolated from E18 embryos) with anti-polySia mAb (12E3)

showed almost the same levels of polySia expression between *Mgat3*^{+/+} and *Mgat3*^{-/-} mice (Fig. 2D). Immunostaining of adult brain sections with the anti-polySia mAb also confirmed the equivalent expression of polySia between adult *Mgat3*^{+/+} and *Mgat3*^{-/-} mice (Fig. 2E). These data reveal that the HNK-1 epitope but not polySia is upregulated in *Mgat3*^{-/-} brain.

Sia and Fuc contents were also increased in Mgat3^{-/-} kidney

To examine whether the above results found in brain are general or more brain-specific, we also analyzed *N*-glycans in kidney by LC-MS (Fig. 3, Supplemental Fig. S3, and Table S2). The number of glycan structures observed was higher in kidney than in brain, and the diagnostic ions for bisecting GlcNAc were again completely disappeared in *Mgat3*^{-/-} kidney (Fig. S3). The sum of signal intensity of fucosylated glycans in MS analysis showed that the number of tetra and penta-fucosylated *N*-glycans was higher in *Mgat3*^{-/-} than in *Mgat3*^{+/+}, whereas that of di- and tri-fucosylated glycans was reduced in *Mgat3*^{-/-} kidney (Fig. 3A). Similarly, non-sialylated glycans were reduced in *Mgat3*^{-/-} kidney, while sialylated glycans were increased (Fig. 3B). These findings are consistent with the results in brain and suggest that loss of bisecting GlcNAc generally leads to increases in terminal modifications of *N*-glycans.

Preferred glycosylation of various glycosyltransferases toward non-bisected N-glycan

The above data revealed that the loss of bisecting GlcNAc causes upregulation of various kinds of terminal modifications of *N*-glycans. To explore the mechanisms behind these observations, the mRNA levels of glycosyltransferases responsible for these terminal modifications were measured. Fig. 3A shows that fucosyltransferases (*Fut1-11*), sialyltransferases (*St3gal1-6*, *St6gal1,2*), HNK-1-synthesizing enzymes (*B3gat1,2*), and polySia-synthesizing enzymes (*St8sia2,4*) were not upregulated in *Mgat3*^{-/-} brain (Fig. 4A). We also measured the levels of donor substrates for those enzymes in mouse brain and observed comparable levels for all donor substrates tested, including GDP-Fuc and UDP-GlcA, in *Mgat3*^{+/+} and *Mgat3*^{-/-} mice (Fig. 4B). These data exclude the possibility that the increased

expression of terminal *N*-glycan modifications in *Mgat3*^{-/-} was caused by upregulation of biosynthetic enzymes or their donor substrates.

Based on these findings, we hypothesized that the presence of bisecting GlcNAc in *N*-glycans interferes with the catalytic activity of the various enzymes for terminal modifications of *N*-glycans and that the loss of bisecting GlcNAc makes *N*-glycans better substrates for those enzymes. To test this possibility, *in vitro* activity assays of those enzymes were performed using two acceptor substrates (galactosylated biantennary *N*-glycans) with or without bisecting GlcNAc (Fig. 4C, D). To prepare a non-bisected substrate, pyridylamine (PA)-labelled *N*-glycan (GnGnbi-PA) derived from the egg yolk glycopeptide (42) was galactosylated by recombinant B4GALT1 (31) (Supplemental Fig. S4A, C) to produce GGnGGnbi-PA. For preparing a bisected substrate, GnGnbi-PA was first incubated with recombinant GnT-III (Supplemental Fig. S4B) and then with B4GALT1 to obtain the bisected GGnGGnbi-PA (bisectGGnGGnbi-PA) (Supplemental Fig. S4C). These two acceptor substrates showed the same retention times as the commercially available glycan standards in reversed-phase HPLC (Supplemental Fig. S4C) and the expected mass by MALDI-MS analysis (Supplemental Fig. S4D). For activity assays toward the prepared substrates, we expressed and purified representative glycosyltransferases responsible for the biosynthesis of the increased terminal modifications in *Mgat3*^{-/-} brain, including FUT1, 2, 4, 9, ST6GAL1, ST3GAL4 and GlcAT-P (major glucuronyltransferase for HNK-1 biosynthesis) (Supplemental Fig. S5). These enzymes were incubated with GGnGGnbi-PA or bisectGGnGGnbi-PA, and the reaction products were separated and detected by reversed-phase HPLC. Their enzymatic activity was measured based on the peak areas of the products (Fig. 4C, D), and we found that all tested enzymes except FUT1 showed lower activity toward the bisected type substrate than toward the non-bisected type substrate. This strongly suggests that the loss of bisecting GlcNAc converts *N*-glycans from non-preferable to preferable substrates of the enzymes for terminal modifications of *N*-glycans, leading to the higher expression levels of Le-fucose, sialic acid and the HNK-1 epitope in *Mgat3*^{-/-} brain.

Intracellular activity of Le-fucosylation enzymes, ST3GAL4 and GlcAT-P, is suppressed by GnT-III overexpression

To verify this possibility, the glycosyltransferases for the terminal modifications of *N*-glycans were overexpressed with or without GnT-III in cultured cells. Overexpression of Le-type fucosylation enzymes, FUT2, FUT4 and FUT9, in Hela cells resulted in dramatic increases in AAL reactivity (Fig. 5A), indicating that the expressed fucosyltransferases actively fucosylated the protein glycans in cells. Such effects of FUT overexpression on AAL reactivity were clearly suppressed by co-expression of GnT-III (Fig. 5A), but not by the inactive GnT-III mutant (D321A) (56) (Supplemental Fig. S6A). These findings are consistent with the MS and lectin blotting results of *Mgat3*^{-/-} brain and confirmed that the presence of bisecting GlcNAc suppresses Le-type fucosylation in cells. In addition, the sialyl Le^x epitope, which can be detected by the specific antibody F2 (57), was synthesized by overexpression of the biosynthetic enzyme, FUT4 or FUT7 (Supplemental Fig. S6B), and the biosynthesis of sialyl Le^x was also suppressed by GnT-III overexpression. These results further confirmed that Le-type fucosylation is negatively regulated by bisecting GlcNAc.

Similar results were observed for ST3GAL4 and GlcAT-P. Overexpression of ST3GAL4 in CHO cells increased slightly MAM reactivity of cellular proteins, and such an effect was reduced by GnT-III overexpression (Fig. 5B). The HNK-1 epitope is not endogenously expressed in most cell lines, including Hela, and overexpression of one of the two glucuronyltransferases (GlcAT-P and GlcAT-S, encoded by *B3GAT1* and *B3GAT2*, respectively) and the sulfotransferase (HNK-1ST encoded by *CHST10*) causes cells to express this epitope (33). The production of HNK-1 in Hela cells was clearly suppressed by GnT-III overexpression (Fig. 5C), again confirming that the presence of bisecting GlcNAc suppresses the action of GlcAT-P in cells. We also knocked down GnT-III expression by siRNA (Supplemental Fig. S7A, B), and confirmed that the effects of overexpression of a fucosyltransferase (FUT2) and GlcAT-P on the production of terminal glycan epitopes were enhanced by GnT-III silencing (Supplemental Fig. S7C, D). These data support our conclusion that the presence of bisecting GlcNAc suppresses the expression of various terminal epitopes of *N*-glycans.

N-glycan with bisecting GlcNAc adopts back-fold conformation and is poorly recognized by glycosyltransferases

To gain insights into the preference of non-bisected glycans over bisected glycans for enzymes acting on *N*-glycan terminals, we conducted a molecular modelling study and examined how these glycans are recognized by glycosyltransferases. Two enzymes, GlcAT-P and ST6GAL1, whose crystal structures are available, were selected (43, 44). The models of the glycan-enzyme complexes were constructed by fitting Gal β 1,4GlcNAc of the α 1,3-branch over the Gal β 1,4GlcNAc glycan fragment present in the human GlcAT-P crystal structure and this complex underwent MD simulations (Supplemental Fig. S8A-F). GlcAT-P complexes with the non-bisected biantennary *N*-glycan (GGnGGnbi) showed binding of the α 1,3-branch to the GlcAT-P acceptor binding site, whereas Gal-6' of the α 1,6-branch formed favorable electrostatic interactions with R162 (Fig. 6A). This suggests that GlcAT-P prefers the α 1,3-branch as an acceptor substrate, which is consistent with the previous enzyme assay showing that GlcAT-P transferred a glucuronic acid to the α 1,3-branch more efficiently than to the α 1,6-branch (60:40 for α 1,3 to α 1,6) (58). In contrast, the α 1,6-branch of the bisected biantennary *N*-glycan (bisectGGnGGnbi) in GlcAT-P complex occupied an extended conformation and the interaction with GlcAT-P was lost (Fig. 6B). In both cases, the side-chain of F245 is involved in stacking interactions with the GlcNAc-5, which is in agreement with a previous study showing that the F245A mutant has no activity (44). Furthermore, high root mean square fluctuations (RMSF) were observed for the remaining residues during the MD simulation (Supplemental Fig. S7G, GlcNAc-1,2, Man-3,4,4'), suggesting higher atomic fluctuations of these residues. This is consistent with the weak electron density of Man-4/Man-4' and no electron density for the remaining core residues in the complex crystal structure (44). Furthermore, as described below, the bisected glycan adopts a back-fold conformation predominantly in which the α 1,6-branch is located distal from the enzyme. These findings indicate that the bisected glycan is weakly recognized by GlcAT-P.

The modelled ST6GAL1/GGnGGnbi complex adopts a conformation similar to that seen in the glycosylation site of its crystal structure (43). The terminal Gal-6 moiety of the α 1,3-branch bound to the acceptor site and formed a stacking interaction with W257 (Fig. 6C). From structural and volume

considerations (both branches are identical); either of the two branches can bind to ST6GAL1, but the α 1,3-branch is likely to be preferred because of favorable polar interactions between Gal-6 and R242 in this binding mode. This is in agreement with a previous report that ST6GAL1 has a preference for the α 1,3-branch (59). In the presence of bisecting GlcNAc, the α 1,6-branch attains a back-fold conformation (Supplemental Fig. S8F) and interacts mainly with the chitobiose core (Fig. 6D). In this case, loss of the polar interaction between Gal-6' and R242 is partially compensated by the polar interaction between Man-4' and R108, but this interaction is likely to be very weak due to the orientation of the O2 hydroxyl away from R108. Thus, the loss of this polar interaction between Gal-6' and the enzyme leads to poor recognition of the substrate.

The back-fold conformation of bisected glycans observed in MD simulations is in line with previous NMR (60), crystallographic (25), and MD simulation studies (49) where bisected *N*-glycans in the unbound state adopt predominantly a back-fold conformation when compared with that of non-bisected *N*-glycans in solution. Because the α 1,6-branch in the back-fold conformation interacts poorly with the enzyme, the dominant back-fold conformation of the bisected glycans is likely to be the major reason for the lower activity of these enzymes toward the bisected glycan. In conclusion, our modelling and MD results indicate that the presence of bisecting GlcNAc converts the *N*-glycan to a poorer substrate by varying the dominant conformation of the glycan and by losing favorable interactions between a non-acceptor branch and an enzyme.

DISCUSSION

In this study, we found that bisecting GlcNAc suppressed the biosynthesis of Le-type fucose, sialic acid and the HNK-1 epitope at *N*-glycan terminals. As terminal modifications, such as fucose, sialic acid and others, were found to be expressed even in bisected *N*-glycans in our analysis and reports from other groups (61, 62), the suppressive effects of bisecting GlcNAc are probably not exclusive. However, such broad suppressive effects have not been found previously for other sugar residues in *N*-glycan,

this is a unique physiological function of bisecting GlcNAc. Furthermore, based on the enzyme assays and MD simulations, we conclude that the suppression of these terminal modifications is attributed to the substrate specificity of the responsible glycosyltransferases, which were found to prefer non-bisected glycans as acceptor substrates. Although the number of available enzyme structures is currently limited, future structural studies and detailed activity assays of the enzymes acting on *N*-glycan terminals would further reveal how these enzymes accept non-bisected and bisected acceptor substrates.

Previous study reported that *N*-glycan structures in *Mgat3*^{-/-} kidneys were almost comparable to those of *Mgat3*^{+/+} kidney (50). The pattern of signal intensity of the detected glycans in the paper was very similar to our present results. However, the number of detected glycans in these two studies was largely different (approx. 20 vs. 100), and sialylated glycans were not analyzed in the paper. In addition, we used LC-MS, while MALDI was used in the previous paper. In general, MALDI lowers sensitivity for sialylated glycans, and LC-MS shows better performance in relative quantification of glycans including sialylated forms. We think that the results in the two studies are basically consistent but reach the different conclusions because of the different methods and sensitivity for glycan analysis.

Our glycomic and lectin blotting results showed that Le-type but not core fucosylation is enhanced in *Mgat3*^{-/-} brain. This seems to be inconsistent with the previous *in vitro* enzymatic assays showing that the core-fucosylation enzyme FUT8 does not prefer bisected *N*-glycan as a substrate (63). Considering that *N*-glycan is generally biosynthesized by step-wise actions of Golgi enzymes, FUT8 action might precede GnT-III in the Golgi and not be affected by GnT-III in an *in vivo* situation. In addition to FUT8, other GlcNAc-branching enzymes, GnT-IV and -V, were also reported to show little or no activity toward bisected *N*-glycans (21, 22), leading to the possibility that the products of these enzymes were also upregulated in *Mgat3*^{-/-} tissues. In our glycomic analysis using mouse brain, however, the expression levels and the number of glycans identified to have a GlcNAc product of GnT-IV or -V were very low, and we cannot conclude whether these branches were increased in *Mgat3*^{-/-} brain. This issue should be solved by more extensive glycomic studies using various knockout mice and cells of *Mgat* genes.

As compared with Le-fucosylation and HNK-1 biosynthesis, the effects of bisecting GlcNAc on sialylation in lectin blots were moderate (Fig. 1E). Moreover, although enzymatic assays and MD simulations clearly showed that ST6GAL1 prefers the non-bisected substrate (Fig. 4D, 6C, D), overexpression of GnT-III did not suppress the action of ST6GAL1 in Hela cells (Supplemental Fig. S9A). This is consistent with previous reports showing that overexpression of GnT-III downregulates α 2,3-sialylation but not α 2,6-sialylation in cancer cell lines (64, 65). Although this could be explained by the action of ST6GAL1 on *O*-glycans, the suppressive effects of GnT-III overexpression on SSA reactivity was not observed even in the presence of the *O*-glycosylation inhibitor, benzyl-GalNAc (Supplemental Fig. S9B). Overexpressed ST6GAL1 in cells might bypass or precede the action of GnT-III to actively sialylate glycoproteins.

Our MD results of α 1,3-binding modes showed that the interaction of ST6GAL1 and GlcAT-P with non-bisected glycans was stronger than with bisected glycans. Consistently, these two enzymes were reported to show stronger activity toward the α 1,3-branch (58, 59); although, the α 1,6-branch is also accepted as a substrate with lower affinity. Thus, we also modelled GGnGGnbi and bisectGGnGGnbi with the two enzymes in the α 1,6-binding modes (not shown). Both enzymes bound the α 1,6-branch of the two glycans, but as the α 1,6-branch tends to flip back in the bisected glycan, this arm will be less accessible to the acceptor site when compared with the α 1,3-branch. The higher activity toward the α 1,3-branch can be therefore attributed to the initial conformation of both branches and how well they are orienting outward in their unbound form to interact with proteins. Overall, our MD simulations suggest that the binding preference of GlcAT-P and ST6GAL1 for non-bisected *N*-glycans is because of a complex entropic and enthalpic interplay contributed by varying conformations of both branches.

Bisecting GlcNAc has been reported to be involved in various physiological phenomena and diseases. In particular, the relevance in AD and cancer was shown using *Mgat3*^{-/-} mice (4, 17), and the absence of GnT-III results in various functional alterations of target proteins *in vivo*. Furthermore, in some cancer cells, aberrant upregulation of the *MGAT3* gene and bisecting GlcNAc was reported (66, 67), which is suggested to cause poor clinical outcomes. Currently, these bisecting GlcNAc-related

phenotypes have been mainly considered as the direct consequences of the presence or absence of the bisecting GlcNAc residue itself, but some of these phenotypes could be caused by secondary effects on other parts of *N*-glycans, such as Le-fucosylation, sialylation and synthesis of other terminal epitopes. Because no other sugar residues in *N*-glycan have been found to have such a broad impact on the biosynthesis of other parts of *N*-glycan, the inhibition of terminal modifications may be a major physiological function of bisecting GlcNAc. A large switch of preferable conformations of whole *N*-glycan by the presence of bisecting GlcNAc observed in NMR, crystal and our MD studies (25, 26, 49) further supports this possibility. In conclusion, the findings in this study will help fully understand the functions of bisecting GlcNAc in cells, which we believe will lead to the elucidation of how mammalian cells regulate the biosynthesis of complex glycoconjugates.

ACKNOWLEDGMENTS

We thank Dr. Hiroto Kawashima (Chiba University) for providing anti-Sialyl Le^x antibody (F2). *Mgat3*-deficient mice were generously provided by Dr. Jamey D. Marth (University of California-Santa Barbara). Biotinylated PhoSL was kindly provided by J-Chemical. We acknowledge ACCC RIKEN, Japan and Irish Centre for High Computing (ICHEC) for providing computational resources. We also thank Ms. Rie Imamaki (The University of Tokyo) for helping make a plasmid for his-ST6GAL1 and Dr. Emi Ito for conducting MALDI-TOF-MS analysis. This work was supported by Grant-in-Aid for Scientific Research (C) to Y.K. [17K07356], Leading Initiative for Excellent Young Researchers (LEADER) project to Y.K. from the Japan Society for the Promotion of Science (JSPS), by Takeda Science Foundation, and by Mochida Memorial Foundation for Medical and Pharmaceutical Research. We thank Edanz Group (www.edanzediting.com/ac) for editing a draft of this manuscript.

DATA AVAILABILITY

All the data that support the findings of this study are available from the corresponding author upon reasonable request. Glycomic raw data for glycan-structure analysis was deposited to the GlycoPOST

(announced ID: GPST000027 for brain, GPST000031 for kidney). URL is <https://glycopost.glycosmos.org/preview/11320112625ce833e26627e> (PIN CODE: 6703) for brain and <https://glycopost.glycosmos.org/preview/20393247305d1dadec71482> (PINCODE: 9008) for kidney.

Author Contributions

Y.K. designed the experiments and wrote the manuscript. S.K.M. and Y.Y. helped prepare a draft manuscript. M.N. carried out mass-spectrometric analyses. S.K.M. and Y.Y. prepared docking models and conducted MD simulations. Y.K., Y.T. and K.S. performed biochemical and cell biological experiments. K.N. analyzed nucleotide sugars. All of the authors have discussed the results, commented on the manuscript and approved submission.

References

1. Varki, A. (2017) Biological roles of glycans. *Glycobiology* 27, 3-49
2. Moremen, K. W., Tiemeyer, M., and Nairn, A. V. (2012) Vertebrate protein glycosylation: diversity, synthesis and function. *Nat Rev Mol Cell Biol* 13, 448-462
3. Ohtsubo, K., and Marth, J. D. (2006) Glycosylation in cellular mechanisms of health and disease. *Cell* 126, 855-867
4. Kizuka, Y., Kitazume, S., Fujinawa, R., Saito, T., Iwata, N., Saïdo, T. C., Nakano, M., Yamaguchi, Y., Hashimoto, Y., Staufenbiel, M., Hatsuta, H., Murayama, S., Manya, H., Endo, T., and Taniguchi, N. (2015) An aberrant sugar modification of BACE1 blocks its lysosomal targeting in Alzheimer's disease. *EMBO Mol Med* 7, 175-189
5. Ohtsubo, K., Chen, M. Z., Olefsky, J. M., and Marth, J. D. (2011) Pathway to diabetes through attenuation of pancreatic beta cell glycosylation and glucose transport. *Nat Med* 17, 1067-1075
6. Granovsky, M., Fata, J., Pawling, J., Muller, W. J., Khokha, R., and Dennis, J. W. (2000) Suppression of tumor growth and metastasis in Mgat5-deficient mice. *Nat Med* 6, 306-312
7. Yoshida, A., Kobayashi, K., Manya, H., Taniguchi, K., Kano, H., Mizuno, M., Inazu, T., Mitsuhashi, H., Takahashi, S., Takeuchi, M., Herrmann, R., Straub, V., Talim, B., Voit, T., Topaloglu, H., Toda, T., and Endo, T. (2001) Muscular dystrophy and neuronal migration disorder caused by mutations in a glycosyltransferase, POMGnT1. *Dev Cell* 1, 717-724

8. Pinho, S. S., and Reis, C. A. (2015) Glycosylation in cancer: mechanisms and clinical implications. *Nat Rev Cancer* 15, 540-555
9. Taniguchi, N., and Kizuka, Y. (2015) Glycans and cancer: role of N-glycans in cancer biomarker, progression and metastasis, and therapeutics. *Adv Cancer Res* 126, 11-51
10. Aebi, M. (2013) N-linked protein glycosylation in the ER. *Biochim Biophys Acta* 1833, 2430-2437
11. Stanley, P., Taniguchi, N., and Aebi, M. (2015) N-Glycans. In: rd, Varki, A., Cummings, R. D., Esko, J. D., Stanley, P., Hart, G. W., Aebi, M., Darvill, A. G., Kinoshita, T., Packer, N. H., Prestegard, J. H., Schnaar, R. L., and Seeberger, P. H., eds. *Essentials of Glycobiology*, pp. 99-111, Cold Spring Harbor (NY)
12. Nishikawa, A., Ihara, Y., Hatakeyama, M., Kangawa, K., and Taniguchi, N. (1992) Purification, cDNA cloning, and expression of UDP-N-acetylglucosamine: beta-D-mannoside beta-1,4N-acetylglucosaminyltransferase III from rat kidney. *J Biol Chem* 267, 18199-18204
13. Kizuka, Y., Nakano, M., Kitazume, S., Saito, T., Saido, T. C., and Taniguchi, N. (2016) Bisecting GlcNAc modification stabilizes BACE1 protein under oxidative stress conditions. *Biochem J* 473, 21-30
14. Kizuka, Y., and Taniguchi, N. (2018) Neural functions of bisecting GlcNAc. *Glycoconj J*
15. Yoshimura, M., Nishikawa, A., Ihara, Y., Taniguchi, S., and Taniguchi, N. (1995) Suppression of lung metastasis of B16 mouse melanoma by N-acetylglucosaminyltransferase III gene transfection. *Proc Natl Acad Sci U S A* 92, 8754-8758
16. Yoshimura, M., Ihara, Y., Matsuzawa, Y., and Taniguchi, N. (1996) Aberrant glycosylation of E-cadherin enhances cell-cell binding to suppress metastasis. *J Biol Chem* 271, 13811-13815
17. Song, Y., Aglipay, J. A., Bernstein, J. D., Goswami, S., and Stanley, P. (2010) The bisecting GlcNAc on N-glycans inhibits growth factor signaling and retards mammary tumor progression. *Cancer Res* 70, 3361-3371
18. Miyagawa, S., Murakami, H., Takahagi, Y., Nakai, R., Yamada, M., Murase, A., Koyota, S., Koma, M., Matsunami, K., Fukuta, D., Fujimura, T., Shigehisa, T., Okabe, M., Nagashima, H., Shirakura, R., and Taniguchi, N. (2001) Remodeling of the major pig xenoantigen by N-acetylglucosaminyltransferase III in transgenic pig. *J Biol Chem* 276, 39310-39319
19. Brockhausen, I., Carver, J. P., and Schachter, H. (1988) Control of glycoprotein synthesis. The use of oligosaccharide substrates and HPLC to study the sequential pathway for N-acetylglucosaminyltransferases I, II, III, IV, V, and VI in the biosynthesis of highly branched N-glycans by hen oviduct membranes. *Biochem Cell Biol* 66, 1134-1151
20. Brockhausen, I., Narasimhan, S., and Schachter, H. (1988) The biosynthesis of highly branched N-glycans: studies on the sequential pathway and functional role of N-acetylglucosaminyltransferases I, II, III, IV, V and VI. *Biochimie* 70, 1521-1533

21. Oguri, S., Minowa, M. T., Ihara, Y., Taniguchi, N., Ikenaga, H., and Takeuchi, M. (1997) Purification and characterization of UDP-N-acetylglucosamine: alpha1,3-D-mannoside beta1,4-N-acetylglucosaminyltransferase (N-acetylglucosaminyltransferase-IV) from bovine small intestine. *J Biol Chem* 272, 22721-22727
22. Gu, J., Nishikawa, A., Tsuruoka, N., Ohno, M., Yamaguchi, N., Kangawa, K., and Taniguchi, N. (1993) Purification and characterization of UDP-N-acetylglucosamine: alpha-6-D-mannoside beta 1-6N-acetylglucosaminyltransferase (N-acetylglucosaminyltransferase V) from a human lung cancer cell line. *J Biochem* 113, 614-619
23. Kizuka, Y., and Taniguchi, N. (2016) Enzymes for N-Glycan Branching and Their Genetic and Nongenetic Regulation in Cancer. *Biomolecules* 6
24. Re, S., Miyashita, N., Yamaguchi, Y., and Sugita, Y. (2011) Structural diversity and changes in conformational equilibria of biantennary complex-type N-glycans in water revealed by replica-exchange molecular dynamics simulation. *Biophys J* 101, L44-46
25. Nagae, M., Kanagawa, M., Morita-Matsumoto, K., Hanashima, S., Kizuka, Y., Taniguchi, N., and Yamaguchi, Y. (2016) Atomic visualization of a flipped-back conformation of bisected glycans bound to specific lectins. *Sci Rep* 6, 22973
26. Fujii, S., Nishiura, T., Nishikawa, A., Miura, R., and Taniguchi, N. (1990) Structural heterogeneity of sugar chains in immunoglobulin G. Conformation of immunoglobulin G molecule and substrate specificities of glycosyltransferases. *J Biol Chem* 265, 6009-6018
27. Priatel, J. J., Sarkar, M., Schachter, H., and Marth, J. D. (1997) Isolation, characterization and inactivation of the mouse Mgat3 gene: the bisecting N-acetylglucosamine in asparagine-linked oligosaccharides appears dispensable for viability and reproduction. *Glycobiology* 7, 45-56
28. Kizuka, Y., Funayama, S., Shogomori, H., Nakano, M., Nakajima, K., Oka, R., Kitazume, S., Yamaguchi, Y., Sano, M., Korekane, H., Hsu, T. L., Lee, H. Y., Wong, C. H., and Taniguchi, N. (2016) High-Sensitivity and Low-Toxicity Fucose Probe for Glycan Imaging and Biomarker Discovery. *Cell Chem Biol* 23, 782-792
29. Kitada, T., Miyoshi, E., Noda, K., Higashiyama, S., Ihara, H., Matsuura, N., Hayashi, N., Kawata, S., Matsuzawa, Y., and Taniguchi, N. (2001) The addition of bisecting N-acetylglucosamine residues to E-cadherin down-regulates the tyrosine phosphorylation of beta-catenin. *J Biol Chem* 276, 475-480
30. Kitazume, S., Tachida, Y., Oka, R., Shirotani, K., Saido, T. C., and Hashimoto, Y. (2001) Alzheimer's beta-secretase, beta-site amyloid precursor protein-cleaving enzyme, is responsible for cleavage secretion of a Golgi-resident sialyltransferase. *Proc Natl Acad Sci U S A* 98, 13554-13559
31. Kouno, T., Kizuka, Y., Nakagawa, N., Yoshihara, T., Asano, M., and Oka, S. (2011) Specific enzyme complex of beta-1,4-galactosyltransferase-II and glucuronyltransferase-P facilitates biosynthesis of N-linked human natural killer-1 (HNK-1) carbohydrate. *J Biol Chem* 286, 31337-31346

32. Kakuda, S., Sato, Y., Tonoyama, Y., Oka, S., and Kawasaki, T. (2005) Different acceptor specificities of two glucuronyltransferases involved in the biosynthesis of HNK-1 carbohydrate. *Glycobiology* 15, 203-210
33. Kizuka, Y., Matsui, T., Takematsu, H., Kozutsumi, Y., Kawasaki, T., and Oka, S. (2006) Physical and functional association of glucuronyltransferases and sulfotransferase involved in HNK-1 biosynthesis. *J Biol Chem* 281, 13644-13651
34. Nakano, M., Saldanha, R., Gobel, A., Kavallaris, M., and Packer, N. H. (2011) Identification of glycan structure alterations on cell membrane proteins in desoxyepothilone B resistant leukemia cells. *Mol Cell Proteomics* 10, M111 009001
35. Kizuka, Y., Nakano, M., Yamaguchi, Y., Nakajima, K., Oka, R., Sato, K., Ren, C. T., Hsu, T. L., Wong, C. H., and Taniguchi, N. (2017) An Alkynyl-Fucose Halts Hepatoma Cell Migration and Invasion by Inhibiting GDP-Fucose-Synthesizing Enzyme FX, TSTA3. *Cell Chem Biol* 24, 1467-1478 e1465
36. Nakano, M., Nakagawa, T., Ito, T., Kitada, T., Hijioka, T., Kasahara, A., Tajiri, M., Wada, Y., Taniguchi, N., and Miyoshi, E. (2008) Site-specific analysis of N-glycans on haptoglobin in sera of patients with pancreatic cancer: a novel approach for the development of tumor markers. *Int J Cancer* 122, 2301-2309
37. Kizuka, Y., Nakano, M., Miura, Y., and Taniguchi, N. (2016) Epigenetic regulation of neural N-glycomics. *Proteomics* 16, 2854-2863
38. Kizuka, Y., Kitazume, S., Okahara, K., Villagra, A., Sotomayor, E. M., and Taniguchi, N. (2014) Epigenetic regulation of a brain-specific glycosyltransferase N-acetylglucosaminyltransferase-IX (GnT-IX) by specific chromatin modifiers. *J Biol Chem* 289, 11253-11261
39. Sugiura, Y., Honda, K., Kajimura, M., and Suematsu, M. (2014) Visualization and quantification of cerebral metabolic fluxes of glucose in awake mice. *Proteomics* 14, 829-838
40. Nakajima, K., Ito, E., Ohtsubo, K., Shirato, K., Takamiya, R., Kitazume, S., Angata, T., and Taniguchi, N. (2013) Mass isotopomer analysis of metabolically labeled nucleotide sugars and N- and O-glycans for tracing nucleotide sugar metabolisms. *Mol Cell Proteomics* 12, 2468-2480
41. Nakajima, K., Kitazume, S., Angata, T., Fujinawa, R., Ohtsubo, K., Miyoshi, E., and Taniguchi, N. (2010) Simultaneous determination of nucleotide sugars with ion-pair reversed-phase HPLC. *Glycobiology* 20, 865-871
42. Takamatsu, S., Korekane, H., Ohtsubo, K., Oguri, S., Park, J. Y., Matsumoto, A., and Taniguchi, N. (2013) N-acetylglucosaminyltransferase (GnT) assays using fluorescent oligosaccharide acceptor substrates: GnT-III, IV, V, and IX (GnT-Vb). *Methods Mol Biol* 1022, 283-298
43. Kuhn, B., Benz, J., Greif, M., Engel, A. M., Sobek, H., and Rudolph, M. G. (2013) The structure of human alpha-2,6-sialyltransferase reveals the binding mode of complex glycans. *Acta Crystallogr D Biol Crystallogr* 69, 1826-1838

44. Kakuda, S., Shiba, T., Ishiguro, M., Tagawa, H., Oka, S., Kajihara, Y., Kawasaki, T., Wakatsuki, S., and Kato, R. (2004) Structural basis for acceptor substrate recognition of a human glucuronyltransferase, GlcAT-P, an enzyme critical in the biosynthesis of the carbohydrate epitope HNK-1. *J Biol Chem* 279, 22693-22703
45. Nivedha, A. K., Thieker, D. F., Makeneni, S., Hu, H., and Woods, R. J. (2016) Vina-Carb: Improving Glycosidic Angles during Carbohydrate Docking. *J Chem Theory Comput* 12, 892-901
46. Li, P., and Merz, K. M., Jr. (2014) Taking into Account the Ion-induced Dipole Interaction in the Nonbonded Model of Ions. *J Chem Theory Comput* 10, 289-297
47. Nagae, M., Mishra, S. K., Hanashima, S., Tateno, H., and Yamaguchi, Y. (2017) Distinct roles for each N-glycan branch interacting with mannose-binding type Jacalin-related lectins Oryzata and Calsepa. *Glycobiology* 27, 1120-1133
48. Case, D. A., Babin, V., Berryman, J. T., Betz, R. M., Cai, Q., Cerutti, D. S., Cheatham, I., T. E., Darden, T. A., Duke, R. E., Gohlke, H., Goetz, A. W., Gusarov, S., Homeyer, N., Janowski, P., Kaus, J., Kolossvary, I., Kovalenko, A., Lee, T. S., LeGrand, S., Luchko, T., Luo, R., Madej, B., Merz, K. M., Paesani, F., Roe, D. R., Roitberg, A., Sagui, C., Salomon-Ferrer, R., Seabra, G., Simmerling, C. L., Smith, W., Swails, J., Walker, R. C., Wang, J., Wolf, R. M., Wu, X., and Kollman, P. A. (2014) *AMBER 14*, University of California
49. Nishima, W., Miyashita, N., Yamaguchi, Y., Sugita, Y., and Re, S. (2012) Effect of bisecting GlcNAc and core fucosylation on conformational properties of biantennary complex-type N-glycans in solution. *J Phys Chem B* 116, 8504-8512
50. Bhattacharyya, R., Bhaumik, M., Raju, T. S., and Stanley, P. (2002) Truncated, inactive N-acetylglucosaminyltransferase III (GlcNAc-TIII) induces neurological and other traits absent in mice that lack GlcNAc-TIII. *J Biol Chem* 277, 26300-26309
51. Wimmerova, M., Mitchell, E., Sanchez, J. F., Gautier, C., and Imberty, A. (2003) Crystal structure of fungal lectin: six-bladed beta-propeller fold and novel fucose recognition mode for *Aleuria aurantia* lectin. *J Biol Chem* 278, 27059-27067
52. Kobayashi, Y., Tateno, H., Dohra, H., Moriwaki, K., Miyoshi, E., Hirabayashi, J., and Kawagishi, H. (2012) A novel core fucose-specific lectin from the mushroom *Pholiota squarrosa*. *J Biol Chem* 287, 33973-33982
53. Kizuka, Y., and Oka, S. (2012) Regulated expression and neural functions of human natural killer-1 (HNK-1) carbohydrate. *Cell Mol Life Sci* 69, 4135-4147
54. Morise, J., Takematsu, H., and Oka, S. (2017) The role of human natural killer-1 (HNK-1) carbohydrate in neuronal plasticity and disease. *Biochim Biophys Acta Gen Subj* 1861, 2455-2461
55. Colley, K. J., Kitajima, K., and Sato, C. (2014) Polysialic acid: biosynthesis, novel functions and applications. *Crit Rev Biochem Mol Biol* 49, 498-532

56. Ihara, H., Ikeda, Y., Koyota, S., Endo, T., Honke, K., and Taniguchi, N. (2002) A catalytically inactive beta 1,4-N-acetylglucosaminyltransferase III (GnT-III) behaves as a dominant negative GnT-III inhibitor. *Eur J Biochem* 269, 193-201
57. Matsumura, R., Hirakawa, J., Sato, K., Ikeda, T., Nagai, M., Fukuda, M., Imai, Y., and Kawashima, H. (2015) Novel Antibodies Reactive with Sialyl Lewis X in Both Humans and Mice Define Its Critical Role in Leukocyte Trafficking and Contact Hypersensitivity Responses. *J Biol Chem* 290, 15313-15326
58. Oka, S., Terayama, K., Imiya, K., Yamamoto, S., Kondo, A., Kato, I., and Kawasaki, T. (2000) The N-glycan acceptor specificity of a glucuronyltransferase, GlcAT-P, associated with biosynthesis of the HNK-1 epitope. *Glycoconj J* 17, 877-885
59. Barb, A. W., Brady, E. K., and Prestegard, J. H. (2009) Branch-specific sialylation of IgG-Fc glycans by ST6Gal-I. *Biochemistry* 48, 9705-9707
60. Homans, S. W., Dwek, R. A., Boyd, J., Mahmoudian, M., Richards, W. G., and Rademacher, T. W. (1986) Conformational transitions in N-linked oligosaccharides. *Biochemistry* 25, 6342-6350
61. Fredriksson, S. A., Podbielska, M., Nilsson, B., Krotkiewska, B., Lisowska, E., and Krotkiewski, H. (2010) ABH blood group antigens in N-glycan of human glycophorin A. *Arch Biochem Biophys* 498, 127-135
62. Klisch, K., Jeanrond, E., Pang, P. C., Pich, A., Schuler, G., Dantzer, V., Kowalewski, M. P., and Dell, A. (2008) A tetraantennary glycan with bisecting N-acetylglucosamine and the Sd(a) antigen is the predominant N-glycan on bovine pregnancy-associated glycoproteins. *Glycobiology* 18, 42-52
63. Longmore, G. D., and Schachter, H. (1982) Product-identification and substrate-specificity studies of the GDP-L-fucose:2-acetamido-2-deoxy-beta-D-glucoside (FUC goes to Asn-linked GlcNAc) 6-alpha-L-fucosyltransferase in a Golgi-rich fraction from porcine liver. *Carbohydr Res* 100, 365-392
64. Lu, J., Isaji, T., Im, S., Fukuda, T., Kameyama, A., and Gu, J. (2016) Expression of N-Acetylglucosaminyltransferase III Suppresses alpha2,3-Sialylation, and Its Distinctive Functions in Cell Migration Are Attributed to alpha2,6-Sialylation Levels. *J Biol Chem* 291, 5708-5720
65. Koyota, S., Ikeda, Y., Miyagawa, S., Ihara, H., Koma, M., Honke, K., Shirakura, R., and Taniguchi, N. (2001) Down-regulation of the alpha-Gal epitope expression in N-glycans of swine endothelial cells by transfection with the N-acetylglucosaminyltransferase III gene. Modulation of the biosynthesis of terminal structures by a bisecting GlcNAc. *J Biol Chem* 276, 32867-32874
66. Klasic, M., Kristic, J., Korac, P., Horvat, T., Markulin, D., Vojta, A., Reiding, K. R., Wuhner, M., Lauc, G., and Zoldos, V. (2016) DNA hypomethylation upregulates expression of the MGAT3 gene in HepG2 cells and leads to changes in N-glycosylation of secreted glycoproteins. *Sci Rep* 6, 24363
67. Kohler, R. S., Anugraham, M., Lopez, M. N., Xiao, C., Schoetzau, A., Hettich, T., Schlotterbeck, G., Fedier, A., Jacob, F., and Heinzelmann-Schwarz, V. (2016) Epigenetic

activation of MGAT3 and corresponding bisecting GlcNAc shortens the survival of cancer patients. *Oncotarget* 7, 51674-51686

Figure 1

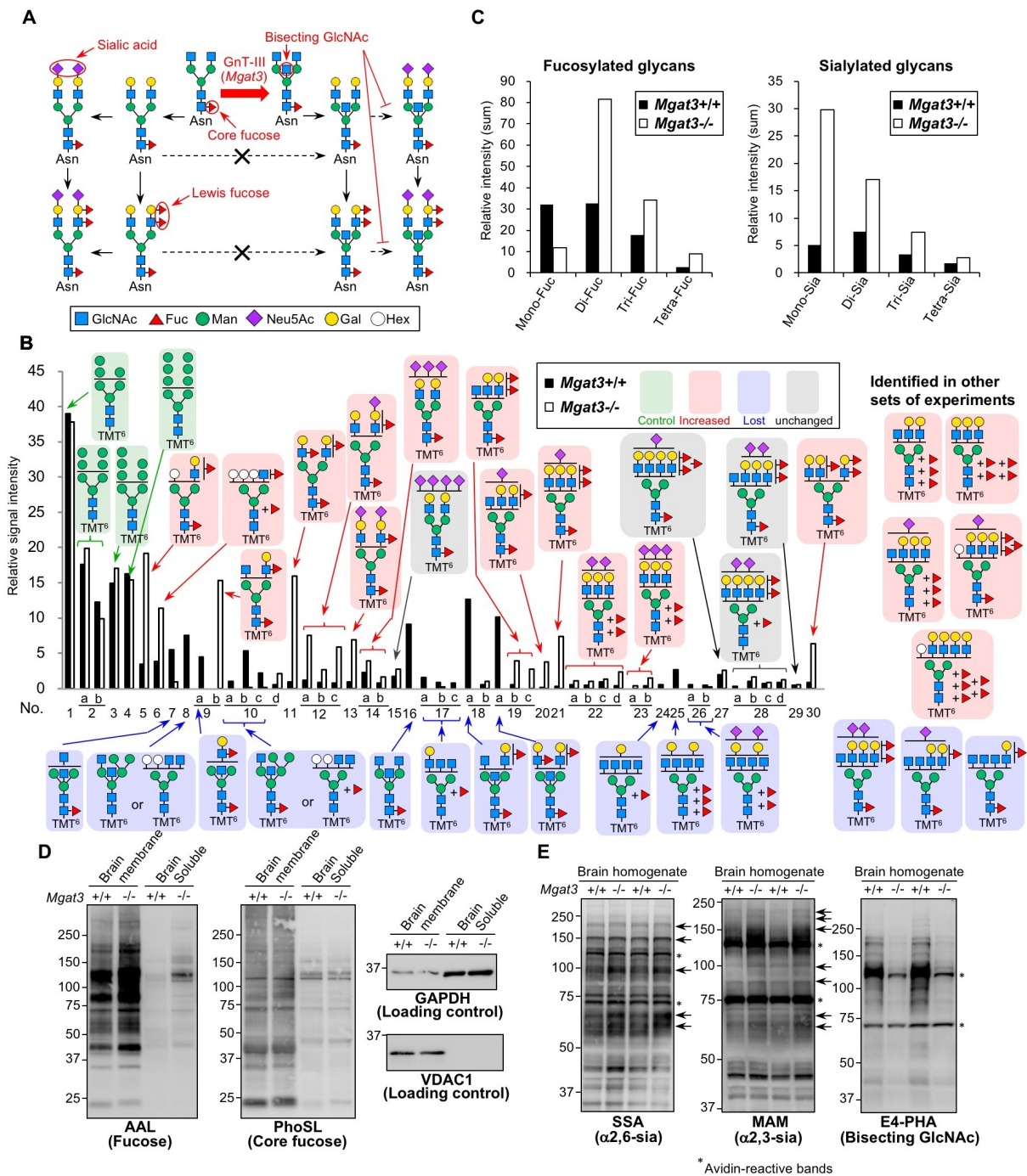


Fig. 1. Enhanced sialylation and Le-fucosylation of *N*-glycans in *Mgat3*^{-/-} brain. (A) A schematic model of GnT-III action, sialylation and fucosylation of *N*-glycans. Presence of bisecting GlcNAc suppresses biosynthesis of sialic acid and Lewis fucose. (B) LC-MS signal intensities of major *N*-glycans derived from adult *Mgat3*^{+/+} and *Mgat3*^{-/-} brains. Green, control oligomannose glycans; pink, glycans increased in *Mgat3*^{-/-}; blue, glycans that disappeared in *Mgat3*^{-/-}; and grey, glycans unchanged between *Mgat3*^{+/+} and *Mgat3*^{-/-}. Fuc, whose position was either core or Lewis, is depicted as + Fuc. 3 independent pairs of *Mgat3*^{+/+} and *Mgat3*^{-/-} brains were analyzed, and we reproducibly found the increases in fucosylated and sialylated glycans in *Mgat3*^{-/-} brain. (C) Sum of signal intensities of mono- and multi-fucosylated (left) and -sialylated (right) glycans in LC-MS analysis. (D) Brain membrane and soluble proteins from 18-week-old *Mgat3*^{+/+} and *Mgat3*^{-/-} mice were stained with lectin (AAL or PhoSL), anti-GAPDH, or anti-VDAC1 Ab. (E) Proteins of brain homogenates from 15-week-old *Mgat3*^{+/+} and *Mgat3*^{-/-} mice were stained with SSA, MAM, or the E4-PHA lectin. The representative

data of two mice for each genotype are shown. Arrows indicate the bands whose signal intensity was prominently increased in *Mgat3*^{-/-} brain. Asterisks indicate non-specific bands reactive with only avidin.

Figure 2

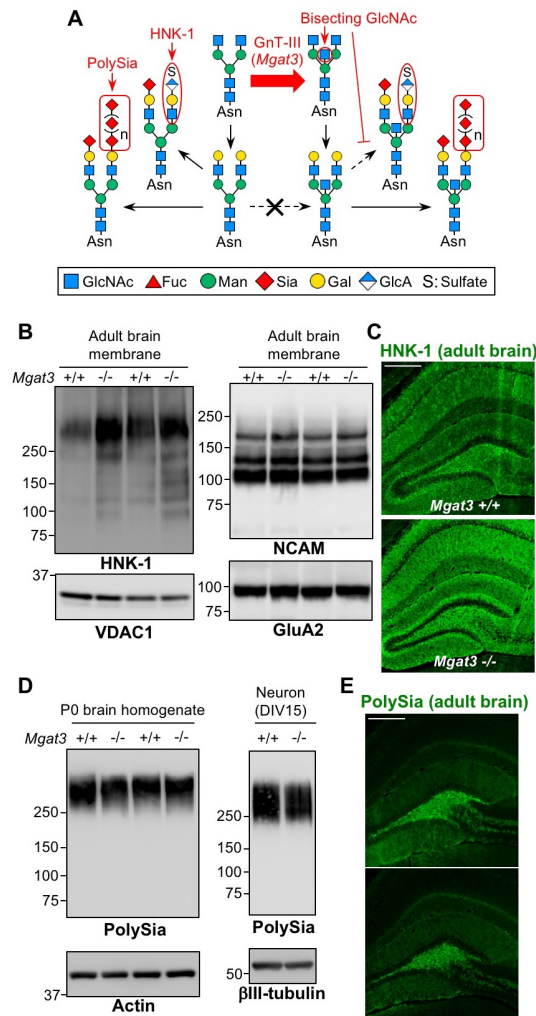


Fig. 2. Increase in the HNK-1 glycan level in *Mgat3*^{-/-} brain. (A) A schematic model describing the biosynthesis of bisecting GlcNAc, HNK-1 and polySia in *N*-glycans. (B) Proteins of brain membranes from 7-week-old *Mgat3*^{+/+} and *Mgat3*^{-/-} mice were stained with the anti-HNK-1, anti-NCAM, anti-GluA2 and anti-VDAC1 Ab. The data of two representative mice for each genotype are shown. (C) Brain sections from 20-week-old *Mgat3*^{+/+} and *Mgat3*^{-/-} mice were immunostained with the anti-HNK-1 mAb. Hippocampus area is shown. Bar, 300 μm. (D) Proteins of brain homogenates from P0 *Mgat3*^{+/+} and *Mgat3*^{-/-} mice (left) or of DIV15 cultured cerebral neurons from *Mgat3*^{+/+} and *Mgat3*^{-/-} embryos (right) were stained with the anti-polySia, anti-actin, or anti-βIII-tubulin (neuron marker) Ab. (E) Brain sections from 20-week-old *Mgat3*^{+/+} and *Mgat3*^{-/-} mice were immunostained with the anti-polySia mAb. Hippocampus area is shown. Bar, 300 μm.

Figure 3

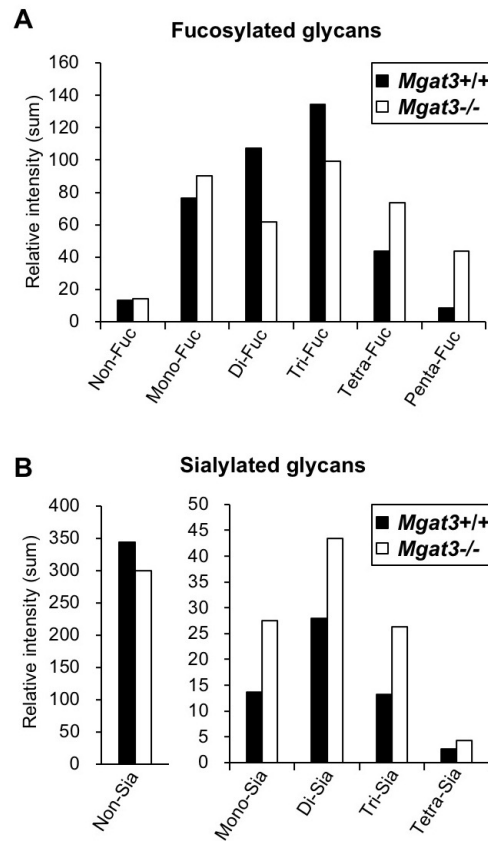


Fig. 3. Enhanced sialylation and Le-fucosylation of *N*-glycans in *Mgat3*^{-/-} kidney. LC-MS signal intensities of *N*-glycans derived from adult *Mgat3*^{+/+} and *Mgat3*^{-/-} kidneys. Sum of signal intensities of non-, mono- and multi-fucosylated (A) and -sialylated (B) glycans in LC-MS analysis is shown.

Figure 4

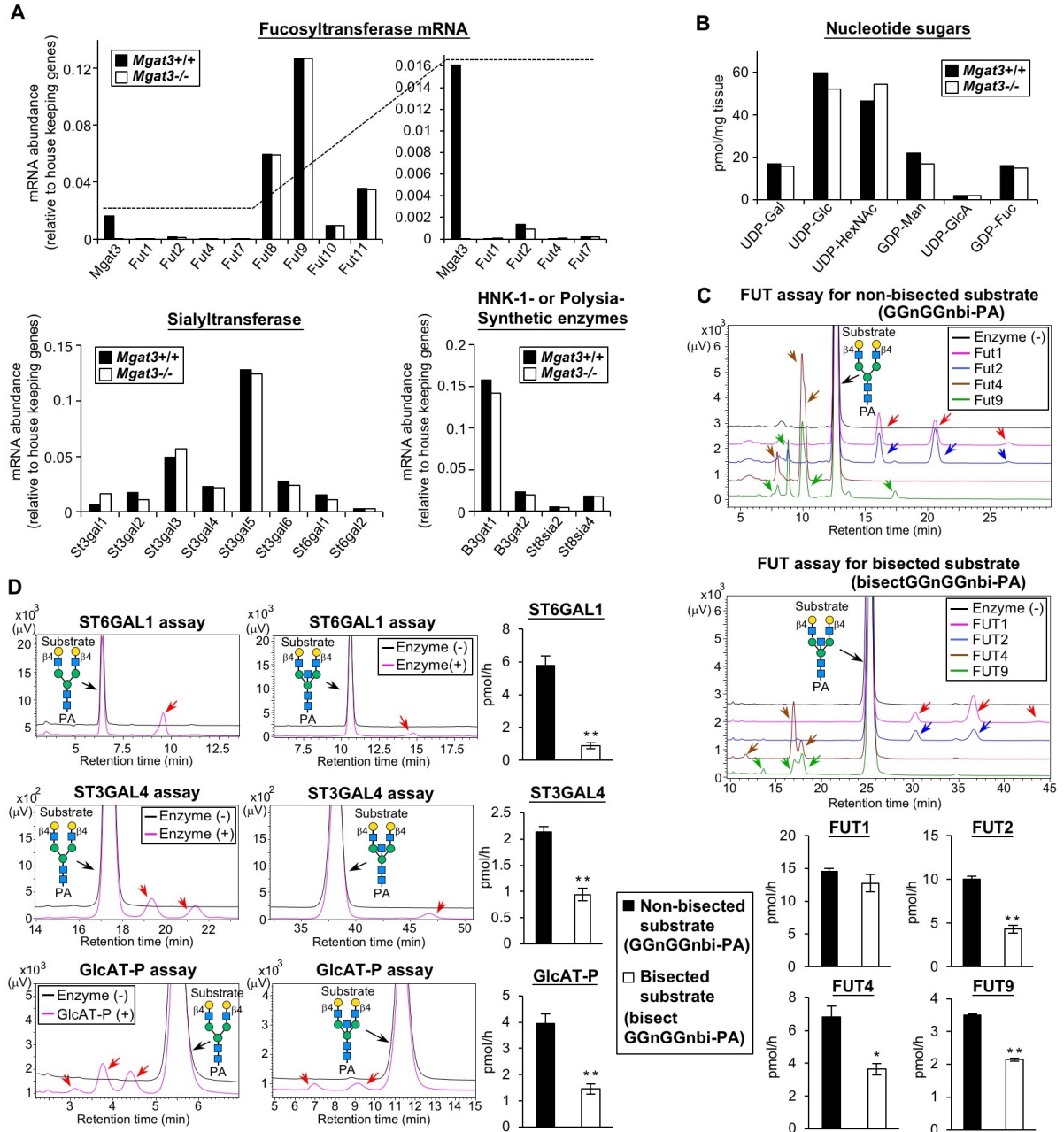


Fig. 4. Preferred glycosylation of various glycosyltransferases toward non-bisected *N*-glycan. (A) The mRNA levels of various glycosyltransferases normalized by house keeping genes in brains from 6-week-old *Mgat3*^{+/+} and *Mgat3*^{-/-} mice were quantified by qPCR ($n = 2$). (B) The levels of various nucleotide sugars in *Mgat3*^{+/+} and *Mgat3*^{-/-} mouse brains were quantified by LC-MS ($n = 1$). (C) *In vitro* enzymatic activity of recombinant FUT1, FUT2, FUT4 and FUT9 toward GGnGGnbi-PA and bisectGGnGGnbi-PA were measured ($n = 3$). (D) Enzymatic activity of recombinant ST6GAL1, ST3GAL4, and GlcAT-P toward GGnGGnbi-PA and bisectGGnGGnbi-PA were measured ($n = 3$). Arrows indicate the products of glycosyltransferase reactions. All graphs show means \pm SEM, and all measurements were taken from distinct samples (* $p < 0.05$, ** $p < 0.01$, Student's *t*-test)

Figure 5

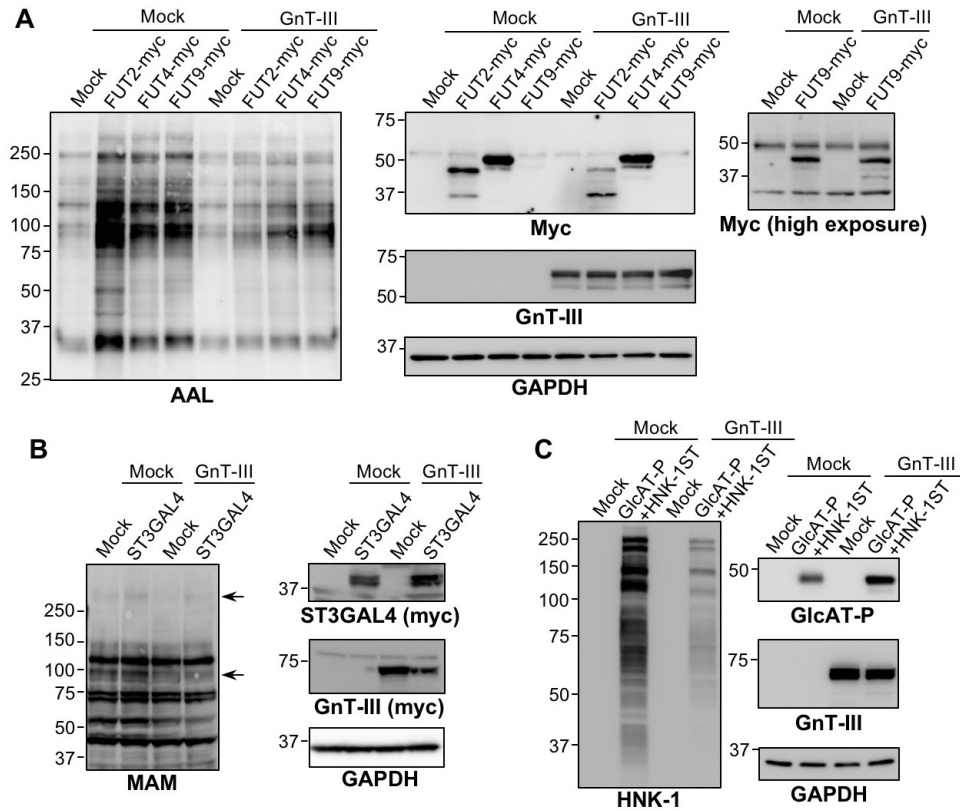


Fig. 5. Intracellular activity of Le-fucosylation enzymes, ST3GAL4 and GlcAT-P, is suppressed by GnT-III overexpression. (A) HeLa cells were transfected with the FUT2-myc, FUT4-myc, or FUT9-myc expression plasmid or the empty vector (mock) with or without the GnT-III expression plasmid. Cellular proteins were stained with the AAL lectin, anti-myc, anti-GnT-III, or anti-GAPDH Ab. A highly exposed myc-blot is also presented to show clearly the expression levels of FUT9. (B) CHO cells were transfected with the ST3GAL4 expression plasmid or the empty vector (mock) with or without the GnT-III expression plasmid. Cellular proteins were stained with the MAM lectin, anti-myc, or anti-GAPDH Ab. (C) HeLa cells were transfected with the expression plasmid for GlcAT-P and HNK-1ST (P + ST) or the empty vector (mock) with or without the GnT-III expression plasmid. Cellular proteins were stained with the anti-HNK-1, anti-GIAT-P, anti-GnT-III, or anti-GAPDH Ab.

Figure 6

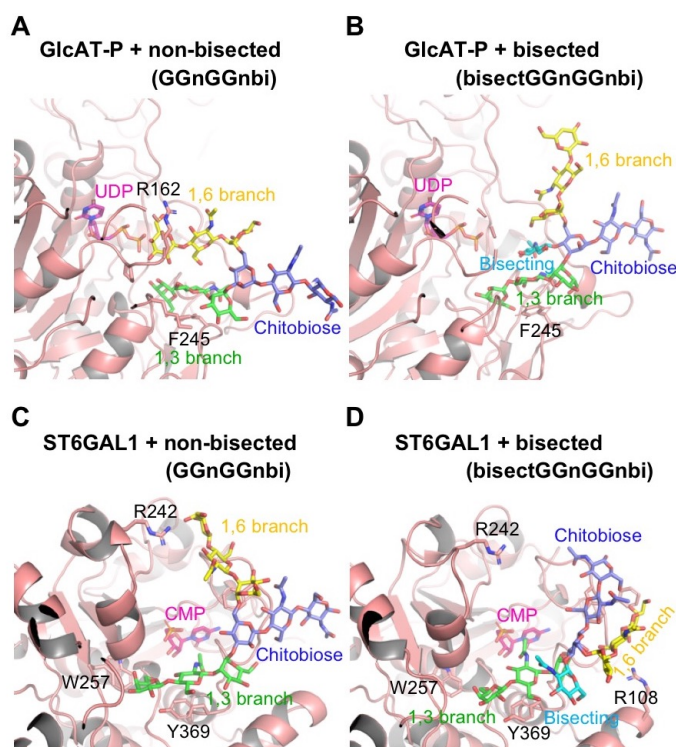


Fig. 6. Binding conformations of bisected and non-bisected *N*-glycans with GlcAT-P and ST6GAL1. Images were taken from the cluster analysis of MD poses and representatives for the most populated clusters are shown. *N*-glycan binding complexes are shown for GlcAT-P (A,B) and ST6GAL1 (C,D) where the chitobiose core (purple), α 1,3-branch (green), α 1,6-branch (yellow) and bisecting GlcNAc (cyan) and relevant side chains (brown) are shown in stick representation. The UDP and CMP molecules in the figure were taken after superimposing the MD structure over the crystal structure. (A) The α 1,6-branch of the biantennary *N*-glycan interacts with GlcAT-P. (B) In the presence of bisecting GlcNAc, the α 1,6-branch cannot interact with GlcAT-P. (C) In ST6GAL1 complex, the α 1,6-branch interacts with the enzyme by forming a hydrogen bond with R242. (D) In the presence of bisecting GlcNAc, the α 1,6-branch obtains a back-fold conformation and interacts with the chitobiose core, lacking favorable interactions between the α 1,6-branch and enzyme.